lubricants

MDPI

Article

A Skid Resistance Predicting Model for Single Carriageways

Miren Isasa [1], Ángela Alonso-Solórzano [2], Itziar Gurrutxaga [1] and Heriberto Pérez-Acebo [3,*]

[1] Mechanical Engineering Department, University of the Basque Country UPV/EHU, Pl. Europa, 1, 20018 Donostia-San Sebastián, Spain; miren.isasa@ehu.eus (M.I.); itziar.gurruchaga@ehu.eus (I.G.)
[2] Department of Physics, University Francisco de Vitoria, Carretera Pozuelo-Majadahonda, km 1.800, 28223 Pozuelo de Alarcón, Spain; angela.alonso@ufv.es
[3] Mechanical Engineering Department, University of the Basque Country UPV/EHU, P° Rafael Moreno Pitxitxi, 2, 48013 Bilbao, Spain
* Correspondence: heriberto.perez@ehu.eus; Tel.: +34-946017820

Abstract

Skid resistance, or friction, on a road surface is a critical parameter in functional highway assessments, given its direct relationships with safety and accident frequency. Therefore, road administrations must collect friction data across their road networks to ensure safe roads for users. In addition, having a predictive model of skid resistance for each road section is essential for an efficient pavement management system (PMS). Traditionally, road authorities disregard rural roads, since they are more focused on freeways and traffic-intense roads. This study develops a model for predicting minimum-available skid resistance, which occurs in summer, measured using the Sideway-force Coefficient Routine Investigation Machine (SCRIM), on bituminous pavements in the single-carriageway road network of the Province of Gipuzkoa, Spain. To this end, traffic volume data available in the PMS of the Provincial Council of Gipuzkoa, such as the annual average daily traffic (AADT) and the AADT of heavy vehicles (AADT.HV), were uniquely used to forecast skid-resistance values collected in summer. Additionally, a methodology for eliminating outliers is proposed. Despite the simplicity of the model, which does not include information about the materials at the surface layer, a coefficient of determination (R^2) of 0.439 was achieved. This model can help road authorities identify the roads for which lower skid-resistance values are most likely to occur, allowing them to focus their attention and efforts on these roads, which are key infrastructure in rural areas.

Keywords: skid resistance; pavement friction; road safety; SCRIM coefficient; pavement management system

Received: 13 June 2025
Revised: 29 July 2025
Accepted: 12 August 2025
Published: 16 August 2025

Citation: Isasa, M.; Alonso-Solórzano, Á.; Gurrutxaga, I.; Pérez-Acebo, H. A Skid Resistance Predicting Model for Single Carriageways. *Lubricants* **2025**, *13*, 365. https://doi.org/10.3390/lubricants13080365

1. Introduction

Road safety is a crucial and strategic concern for highway authorities worldwide [1–4]. It is widely recognized that road accidents are multifactorial phenomena, involving a variety of elements, including driver behavior, vehicle conditions, and the state of the road infrastructure [5,6]. However, recent research has shown a direct correlation between pavement surface properties and accident rates [7–9]. Moreover, it is worth noting that, of all these factors, road condition represents the only parameter that can be directly intervened upon by the administrations responsible for road management. This makes it a key aspect in strategies aimed at reducing road accidents.

When referring to the condition of the road pavement, it is necessary to have an indicator that allows for its objective evaluation. In this context, it is common to use

parameters related to the friction or skid resistance of the pavement, which are fundamental measures to characterize its ability to interact with tires and, thus, its influence on road safety [10]. Enhanced friction at this interface improves a driver's ability to maintain control of their vehicle [11–13]. On the other hand, a reduction in pavement friction, particularly under wet conditions, has been associated with an increased rate of wet-weather crashes [14,15]. Consequently, it is imperative for highway agencies to ensure that their road networks maintain adequate friction levels [16].

Pavement friction is defined as "the force that resists the relative motion between a vehicle tire and a pavement" [8]. It is the outcome of a complex interaction between adhesion and hysteresis. The former refers to the molecular bonding at the tire–pavement interface associated with the micro-level asperities of the pavement, or micro-texture. The latter is the energy loss due to tire deformation as it interacts with the surface texture and it is related to the macro-level asperities, or macro-texture. Pavement surface texture refers to the deviations from a perfectly planar surface [17–19]. The scales of surface texture were defined by the World Association (PIARC) at the XVII World Road Congress, held in Brussels, in 1987, as a function of the wavelength (λ) and amplitude (A) of these deviations (Table 1) [20].

Table 1. Classification of surface textures.

Texture Level	Wavelength, λ (mm)	Amplitude, A (mm)
Micro-texture	$0 < \lambda < 0.5$	$0.01 < A < 0.5$
Macro-texture	$0.5 < \lambda < 50$	$0.1 < A < 20$
Mega-texture	$50 < \lambda < 500$	$1 < A < 50$
Roughness or unevenness	$\lambda > 500$	$1 < A < 200$

Micro-texture is determined by the surface characteristics of the aggregates and the bituminous material that ensures adhesion. Macro-texture, on the other hand, depends on the mixture properties of the asphalt, including the shape, size, and gradation of the aggregates [21]. While micro-texture and macro-texture are essential for pavement performance, mega-texture and excessive roughness should be avoided [22]. Factors influencing pavement friction are generally categorized into four groups (Table 2) [8,19,23,24].

Table 2. Factors influencing pavement skid resistance.

Pavement Surface Characteristics	Vehicle Factors	Tire Properties	Environment
1. Micro-texture 2. Macro-texture 3. Material properties 4. Mega-texture/ unevenness 5. Temperature	Slip speed, as a function of: 1. Vehicle speed 2. Slip ratio 3. Driving maneuver 3a. Turning 3b. Overtaking	1. Tread design and condition 2. Inflation pressure 3. Rubber composition and hardness 4. Foot print 5. Load 6. Temperature	1. Temperature 2. Water (rainfall, condensation) 3. Snow and ice 4. Contaminants (salt, sand, dirt, mud) 5. Wind

Pavement friction at the network level is usually measured using specialized devices such as a SCRIM (Sideway-force Coefficient Routine Investigation Machine), Mu-Meter, or the GripTester, which allow for the coefficient of friction to be obtained under controlled conditions, both wet and dry [25]. These measurements provide values that can be compared with thresholds established by national and international standards. A coefficient of friction below certain critical limits may indicate an increased risk of loss of vehicle control, especially in adverse weather conditions.

The device established in Spain to measure the skid resistance of a road surface is the SCRIM, which was developed by the Transport and Road Research Laboratory (TRRL) in the United Kingdom to measure sideways force. For SCRIM testing, the equipment is mounted on a truck chassis with a standardized test wheel positioned centrally between the front and rear axles. The wheel is fixed at an angle of 20 degrees to the chassis line and is connected to a water supply. As the truck moves forward, the test wheel rotates but experiences lateral sliding due to the angular difference. The standard testing speed for the SCRIM device is 50 km/h. The SFC, obtained from the SCRIM, is the ratio of the sideways force to the vertical reaction between the tire and the pavement surface, with values ranging from 0 to 1. An SCRIM reading (*SR*) represents the output for each subsection of the tested highway, typically 5, 10, or 20 m in length. It is calculated as the average SFC value across the subsection, expressed as an integer, and multiplied by 100. These SR values are directly generated by the SCRIM machine and must be adjusted for speed. When the truck-mounted SCRIM system replaced the motorbike-mounted versions, an "index of SFC" factor was introduced to correlate historical records with current measurements, ensuring consistency in the data. In the UK, this index is set at 0.78 and applies to all SCRIM devices in use [26]. As a result, the SCRIM coefficient (SC) is calculated for each subsection with a valid SR using Equation (1).

$$SC = (SR(50)/100) \cdot 0.78 \quad (1)$$

The SC is an adjusted SFC value, corrected for speed and machine variability. It is expressed as a decimal fraction, accurate to two decimal places. According to Spanish standards, SC values are expressed on a scale from 0 to 100, by multiplying the value by 100 [27]. The SCRIM coefficient is adjusted for temperature and speed, but no "SFC index" is applied. During testing, all measurements adhere to established standards, with primary considerations including tire properties, water supply, vehicle speed, and slip ratio. Once a road agency selects a specific device for data collection, pavement surface characteristics and environmental factors become the only variable elements, while other factors, as outlined in Table 2, are kept constant to the greatest extent possible.

Systematic monitoring of surface friction, therefore, not only allows for the functional condition of the pavement to be assessed but is also a key tool for planning preventive and corrective maintenance interventions aimed at ensuring adequate safety conditions of the road network.

The behavior of skid resistance over time has been extensively analyzed, leading to the development of an internationally accepted model to represent its performance as pavements age (Figure 1a) [28,29]. This model reflects the influence of factors, such as traffic-induced polishing, environmental conditions, and material properties, providing a standardized framework for predicting and managing skid resistance throughout the pavement's service life. The evolution of skid resistance on newly constructed pavements follows a distinct pattern. Initially, a bituminous film covering the aggregates results in relatively low skid resistance. However, as this film is worn away by traffic, the micro-texture of the aggregates is exposed, leading to a rapid increase in skid resistance. Following this peak, the surface undergoes a polishing phase characterized by a high initial rate of skid-resistance loss, driven by the interaction of traffic with the exposed aggregate. Over time, this rate slows, and the pavement reaches an equilibrium phase where skid resistance stabilizes at an asymptotic value determined by the inherent properties of the aggregates and the level of traffic polishing [29,30]. At this equilibrium phase, seasonal and short-term variations are the only fluctuations. Nevertheless, there is no established consensus regarding the duration of each phase. The duration of the polishing phase, depends on the binder type, its quantity, and the characteristics of heavy traffic [31,32]. In Spain, the initial increase typically lasts between 2 and 3 months [32,33]; however, in other countries, this

period can extend up to 4 years due to the durability of polymer-modified bitumen [34]. Variations in the duration of the polishing phase have also been reported, ranging from 4 to 5 years [35] to one year [29,33].

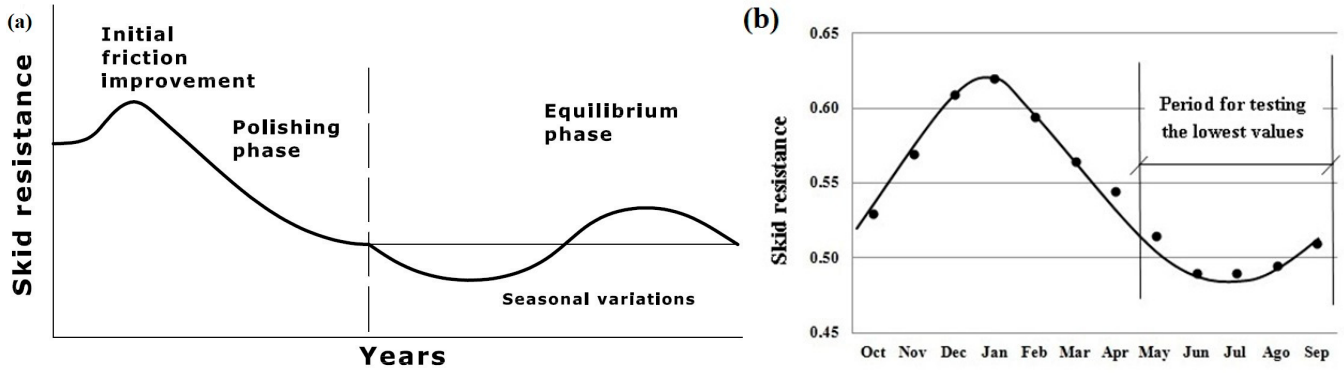

Figure 1. Skid-resistance variation: (**a**) at the beginning; (**b**) seasonal variations.

Seasonal variations in skid resistance have been widely documented, with lower values typically observed on dry road surfaces during summer [36,37]. This is due to the combined effects of increased rubber resilience and reduced hysteresis losses on dry pavements at high temperatures. In contrast, during winter, prolonged wet conditions allow surface aggregates to recover some of their texture and harshness (Figure 1b). These variations are influenced by factors such as the geological history and petrography of the aggregates, as well as traffic intensity, particularly from heavy vehicles, which contribute significantly to the polishing effect. Numerous studies have demonstrated that seasonal variations are most pronounced in pavements during the equilibrium phase [33,38–40]. To account for these fluctuations, road agencies often conduct friction assessments in summer when skid resistance values are at their lowest, ensuring safety by addressing the most adverse conditions in PMS.

Annual variations are primarily influenced by climate changes, although seasonal variations in skid resistance have a more substantial impact.

The degree of polishing is directly correlated with traffic intensity, particularly the volume of heavy traffic [35,41]. It has been reported that, under equal conditions, roads with higher volumes of heavy vehicles tend to exhibit the lowest skid resistance [42]. Heavy traffic contributes to the erosion of fine-scale micro-texture, and an increased presence of heavy vehicles results in a reduction in skid resistance [38]. This relationship is illustrated in Figure 2a, based on research conducted in the UK with aggregates having a PSV between 58 and 60 [40]. The initial decrease in the skid resistance coefficient is attributed to the polishing phase, which stabilizes once the equilibrium phase is reached. Consequently, the effect of heavy traffic should not be considered cumulative over successive years, as it is primarily influenced by traffic intensity and aggregate properties, assuming consistent weather conditions [28,32,35,43]. However, if the intensity of heavy traffic fluctuates—such as changes in the annual average daily traffic (AADT)—the available skid resistance may also vary, potentially increasing, as observed on the A4 road in Colnbrook (UK) when a new freeway was introduced [43] (Figure 2b). A similar phenomenon was also observed on the N-VI in León, Spain [32].

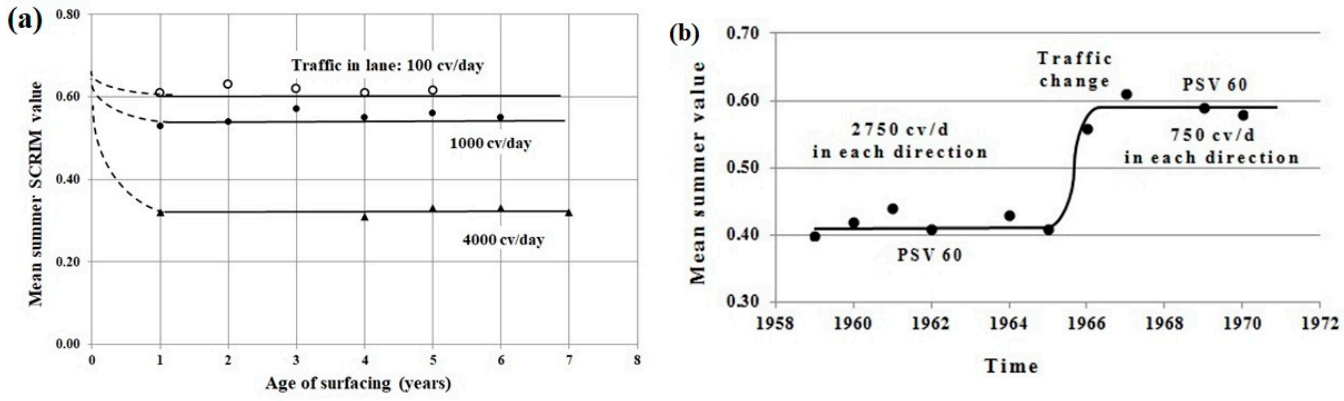

Figure 2. Mean summer SCRIM coefficient (MSSC) variation: (**a**) with constant heavy traffic; (**b**) with changing heavy traffic volume.

As shown, pavement skid resistance is a key characteristic for any pavement management system (PMS) due to its close relationship with road safety, resulting in a parameter that must be monitored by highway administrations in any PMS [44]. Pavement management systems can be defined as "*a set of tools or methods that assist decision makers in finding the optimum strategies for providing, evaluating, and maintaining pavements in a serviceable condition over a period*" [10]. They rely upon three key factors: (1) pavement information and evaluation, (2) pavement performance predicting models to forecast future condition, and (3) development of maintenance and rehabilitation (M&R) plans at the network and project levels, considering local characteristics [45–47]. The development of pavement performance or deterioration models has become a hot topic in pavement management [48], attracting researchers' interest, with a great variety of model types for each index or parameter [3,46,49].

More specifically, regarding skid-resistance prediction, some researchers have addressed the temporal evolution of the friction coefficient [37,50]. Additionally, some studies present skid-resistance prediction models based on real road data [51]. However, the review of the literature allowed us to observe that, in most cases, apart from traffic volume, some aggregate properties are also included as variables in the modeling. These features can be registered in the PMS if the roads are constructed or rehabilitated in recent years. However, in the case of rural roads with a single carriageway in both directions, that information is generally missing or is not properly introduced in the PMS. They are old roads, constructed a long time ago, and they have been rehabilitated in short segments (of around one kilometer or less and sometimes even hundreds of meters), depending on the detected defaults. Therefore, there is a lack of detailed information on every maintenance project. Moreover, those M&R activities cover a wide range of possible solutions, and, hence, they show very different evolution patterns over time. Furthermore, predictive models developed when more information is available show reduced accuracy when extrapolated to the more variable and less controlled contexts of secondary roads.

In light of these considerations, there is a pressing need to advance the understanding of the deterioration dynamics of single-carriageway roads in order to improve predictive capabilities and design more effective maintenance strategies to preserve surface friction and ensure user safety. Consequently, taking the characteristics of secondary roads into consideration, a tailored performance prediction model is necessary for this type of road. As commented, pavements along rural roads are divided in multiple different pavement structures, which usually are not properly included in the PMS. This handicap leads to the development of simplified models using features that were correctly registered in the database, such as traffic volumes. Thus, an adequate solution is provided to overcome the

difficulty of modeling secondary roads with multiple features by means of a simplified but effective approach.

This study aims to create a deterioration model capable of predicting available skid resistance on asphalt concrete single-carriageway roads in Gipuzkoa, Spain. Factors potentially influencing skid resistance are analyzed, with only those demonstrating significant effects incorporated into the model. Such a model would enable the Road Agency of the Provincial Council of Gipuzkoa (PCG) to forecast the friction conditions of its road network and implement proactive measures accordingly.

2. Literature Review

Szatkowski and Hosking [43] developed the earliest study on skid-resistance-prediction models in the UK Transport and Road Research Laboratory (TRRL). This pioneering study analyzed the dependence of the MSSC value on the traffic and the aggregate characteristics, introducing the number of commercial vehicles per day and the PSV, respectively.

That study was considered a "major advancement in the field of skid resistance" [40,52], as it enabled not only the prediction of skidding resistance, but it also provided a framework for estimating the properties of aggregates required to achieve a desired level of skid resistance under specified commercial traffic conditions [40]. It became fundamental to the establishment of standards for road construction in the UK.

From that study onward, different authors have proposed numerous models. Li et al. [53] studied the degradation of friction over time, taking into account the traffic volume and the roadway features. Instead of using the annual average daily traffic to model the SC, Rith et al. [54] used the cumulative traffic on cement concrete pavements together with the road lane. A model for predicting the friction in a complete asphalt road network was proposed, including single-carriageway and double-carriageway roads [55]. Perez-Acebo et al. [56] presented a model for motorways in Bavaria, which depended on traffic volumes and the considered lane and the total number of lanes (2 or 3 per direction). Galvis Arce et al. [57] and Fülöp et al. [58] modeled the deterioration of pavement skid resistance using Markov chains. Other authors, such as Cenek et al. [59], studied the influence of traffic together with the pavement aggregates to analyze the deterioration of the pavement. Nicolosi et al. [51] innovated with a model that included a traffic damage criterion, which incorporated data about traffic volumes, vehicle composition, and motion conditions, verified on an urban motorway with open-graded bituminous surface course. Most of these works were conducted on highways (two-lane roads) and usually on asphalt concrete pavements.

Some studies, including the modeled parameter, independent variables, and the type of road, are summarized in Table 3.

Table 3. Proposed models for predicting skid resistance.

Authors	Model	R^2
Szatkowski and Hosking [43]	$MSSC = 0.024 + 0.663 \cdot 10^4 \cdot Q_{CV} + 1 \cdot 10^{-2} \cdot PSV$ (2)	0.92
WDM Ltd. [60]	$SFC_{50} = 0.018 + 0.311 \cdot 10^4 \cdot Q_{CV} + 0.637 \cdot 10^{-2} \cdot PSV$ (3)	0.28
Cenek et al. [59]	$MSSC = 0.013 \cdot PSV + 0.1 \cdot e^{CHCV} - 0.007 \cdot ALD + 0.44$ (4)	0.38
Perez-Acebo et al. (2020) [55]	$MSSC = 78.497 - 2.321 \cdot \mathrm{LnAADT} + A_L + B_S + C_L \cdot LnAADT$ (5)	0.696
Perez-Acebo et al. (2023) [56]	$GRI_m = 4.33 - 0.344 \cdot LnAADT - 0.260 \cdot LnAADHT + A + B \cdot LnAADT + C \cdot AADT.HV + 0.166 \cdot LnAADT \cdot LnAADT.HV$ (6)	0.405
Rith [54]	$LogSN_{40,Age} = LogSN_{40,i} - 0.07235 \cdot e^{-1.081 \cdot N} \cdot LogCTV$ (7)	0.81

MSSC is the mean summer SCRIM coefficient; Q_{CV} is the number of commercial vehicles per lane per day; PSV is the polished stone value of the aggregate; SFC_{50} is the mean summer SCRIM coefficient measured at 50 km/h; CHCV is the cumulative heavy commercial-vehicle traffic per lane in millions; ALD is the average least dimension of the chip, in mm; AADT is the annual average daily traffic in both directions; A_L is a coefficient that considers the type of road (single- or double-carriageway); B_S is a coefficient that considers the surface layer material; C_L is a coefficient that considers the number of lanes per direction; GRI_m is the mean GRIM value of the segment; AADT.HV is the average annual daily traffic of heavy vehicles in both directions; A, B, and C are coefficients that consider the relative position of the carriageway; $SN_{40,Age}$ is the long-term skid value; $SN_{40,i}$ is the initial skid value; N is the lane number; CTV is the cumulative traffic volume.

Although studies have explored the effects of new materials, mixture designs, and aggregate properties on skid-resistance evolution, as well as models predicting its evolution under controlled conditions [61–63], research using real pavement data remains limited. Specifically, very few models exist that can predict the minimum-available skid resistance of road networks based on data collected directly from in-service pavements (Table 3). Nevertheless, those models need the input of some data, such as aggregate properties, that are not available for rural roads with a single carriageway in both directions. Generally, information for rural roads are not as detailed as for motorways or recently constructed single-carriageway roads. Additionally, the present attention given to pavement skid-resistance prediction is focused on predicting available friction based on three-dimensional (3D) laser-texture measurement devices, which require expensive technology [4,22,64–70]. Furthermore, these kinds of devices are only able to obtain friction values based on texture data but cannot forecast future available skid resistance.

According to the reviewed literature, it is necessary to develop a model for predicting the available friction on rural roads, which are rehabilitated in several segments and for which, generally, there is a lack detailed information. Incorporating relevant factors from previous studies, this research aims to develop a skid-resistance-prediction model for single-carriageway roads in Gipuzkoa, Spain, utilizing the data available in the road agency's PMS. Despite its simplicity, the model is based on key influencing factors and can help highway agencies determine approximate friction values on their road network.

3. Pavement Management System of the Provincial Council of Gipuzkoa

Gipuzkoa is one of the three provinces in the autonomous region of the Basque Country in northern Spain. It is the smallest province of Spain, with a surface area of 1997 km^2 and approximately 726,000 inhabitants. The Basque Country has a unique administrative framework within Spain, granting each province specific authority over road infrastructure. Accordingly, the Provincial Council of Gipuzkoa (PCG) oversees the planning, design, construction, maintenance, funding, and management of the interurban road network within the province, encompassing more than 1300 km of roads. Urban streets are excluded from this network, as each municipality manages them.

In Gipuzkoa, the road network is composed of two main types of roads: separated carriageways roads and single-carriageway roads. The latter represents the vast majority, with a significant portion of the provincial network consisting of conventional roads, accounting for precisely 78% of the road network. However, a notable proportion of the

road infrastructure, especially highways and major routes, are equipped with separated carriageways, which are designed to improve traffic safety and efficiency.

The PCG compiles traffic data, including the average annual daily traffic (AADT) and the percentage of heavy vehicles, enabling the calculation of the AADT for heavy vehicles (AADT.HV). These data consider both directions of the road. This information is published annually online [71]. According to Spanish regulations, heavy vehicles are defined as those exceeding 3500 kg in weight [72].

Additionally, the PCG incorporates environmental data into its PMS. However, due to the relatively small size of Gipuzkoa and its uniform oceanic climate across the region, climatic data were excluded from the model. This decision aligns with standard practices, as small areas with homogeneous climates exhibit minimal environmental variability, which, generally, does not significantly influence regional pavement modeling [73].

For the evaluation of pavement friction conditions, the PCG commonly uses the SCRIM equipment defined before. However, some of the data were collected using a GripTester. This device, following the UNE-CEN/TS 15901-7:2010 IN standard [74], measures pavement friction using a partially locked longitudinal measuring wheel with a fixed sliding degree. From these measurements, the grip number (GN) is obtained and can be correlated with the SC obtained from SCRIM measurements using Equation (8):

$$SC_{SCRIM} = \frac{0.89 \cdot GN}{0.78} \quad (8)$$

Equation (8), developed by the Transport Research Laboratory of the United Kingdom, establishes a correlation of 0.97 between both parameters.

Data collection campaigns were conducted across the entire road network in the years 2005, 2007, 2010, 2018, 2019, 2020, and 2021. For 2005, 2007, 2010, and 2018, the majority of measurements occurred during the winter months (November and January), when friction levels typically reach their peak (Figure 1b). In contrast, the data from 2019, 2020, and 2021 were collected during summer, specifically between May and September, a period characterized by lower friction values and minimal variability (Table 4). SCRIM coefficients were recorded at intervals of 10 meters along the road network, with exact kilometer markers (KPs) noted for both the start and end points. On single-carriageway roads, measurements were taken from one of the two lanes, although the specific lane is not identified.

Table 4. Number of segments included in the modeling for each year.

Year	Number of Segments
2019	22
2020	20
2021	24
TOTAL	66

4. Analysis Methodology

Various prediction models have been discussed in the literature, with deterministic and probabilistic approaches receiving the most attention [75,76]. The skid-resistance models reviewed in Section 3 predominantly belong to the deterministic category. For this study, a deterministic model was chosen, specifically one based on multiple linear regression (MLR). Unlike artificial neural network (ANN) models, which are often regarded as "*black-box*" approaches [46,76–79], deterministic models offer the advantage of clearly identifying and understanding the factors that significantly influence the dependent variable. Other MLR

models obtained good enough accuracy when predicting skid resistance [51,55,56], and we wanted to replicate that successful methodology.

MLR is a statistical method designed to examine the relationship between a dependent variable and several independent variables, typically quantitative in nature. The primary objective of MLR is to use the values of the independent variables to predict the outcome of the dependent variable. The application of MLR relies on several key assumptions that must be satisfied for the model to produce valid results [80].

In this study, MLR was conducted to examine the relationship between the dependent variable and the potential independent variables that could influence this value. The dependent variable to be predicted is the SC measured in summer (mean summer SC, MSSC), defined as the mean value of a segment with the same traffic volume, material for the surface bituminous layer, and age of the pavement.

However, since, in this study, detailed information regarding the age or materials of the surface layers is unavailable, each segment is only defined by areas with the same traffic volume. Therefore, in these segments, which were determined by a traffic-counting device (TCD) and ranged from hundreds of meters to several kilometers long, many SC values are measured. From all of these measurements, a mean SC value, together with the standard deviation, was calculated for each segment (Figure 3a).

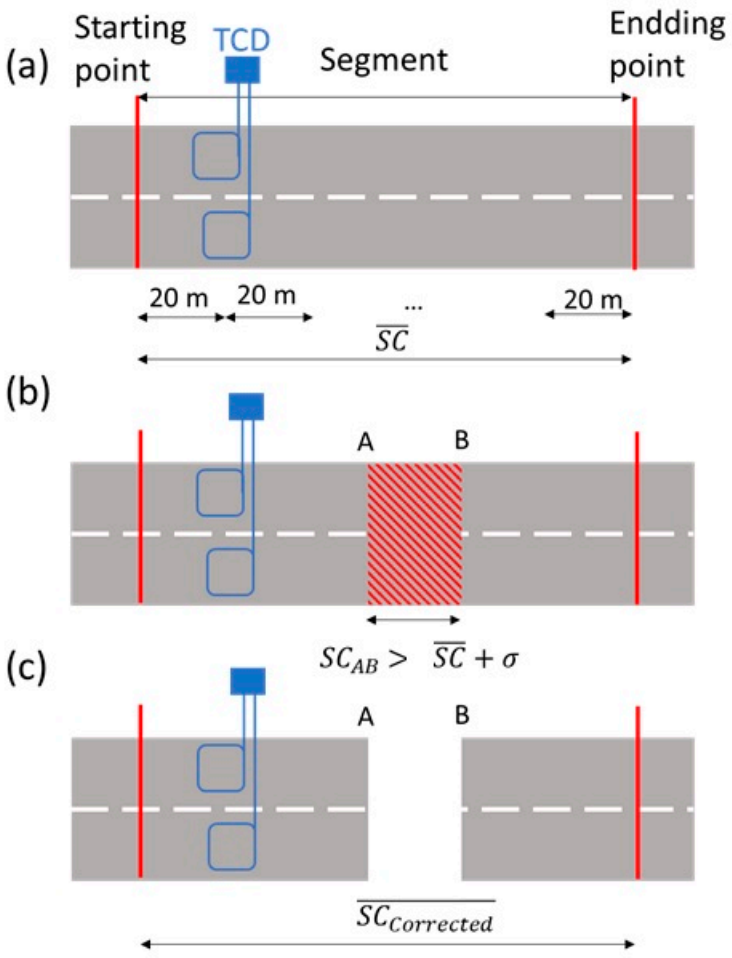

Figure 3. Method used to obtain the mean value of the SC: (**a**) single-carriageway road used to obtain the mean SC value in a segment; (**b**) striped area AB represents an area where the SC exceeds the mean by more than one standard deviation; (**c**) mean SC was recalculated without taking into account the higher SC values between A and B.

In order to identify possible rehabilitated areas for which no intervention was recorded, the following analysis was performed. First, the mean SC was calculated for the whole segment, as defined by the PGC and with a TCD determining the traffic volume for the entire length. Then, each SC value of the segment was compared to the mean SC, adding the standard deviation. If the SC value at a point exceeds the mean by more than one standard deviation, it is assumed that these high-SC-value data correspond to road segments that have undergone repair within the last two years, and, hence, the segment is not in the equilibrium phase, as presented in Figure 2a. In Figure 3b, the red striped area corresponds to points where the SC is greater than the mean SC plus the standard deviation. This methodology was adopted after observing the evolution of the friction values after the application of a new layer up to several years afterward on the roads of Gipuzkoa [33]. It was estimated that the possible variation from summer to winter related to seasonal variations (Figure 1b) could be lower than one standard deviation from the average value in summer, and any value exceeding this limit implies that the polishing phase is not finished (Figure 1a). The literature review clearly identified new surface layers with higher friction values, both in laboratory tests [81,82] and on real roads [50,51]. The results after applying this methodology showed that subsegments of variable lengths were identified, for example, 30 subsegments of 10 m, representing a recently rehabilitated stretch of 300 m, instead of individual 10 m long subsegments randomly distributed over the length of the segment with the same traffic volume. Therefore, the method was qualified as adequate because it was able to clearly identify recently maintained stretches of the road, which showed significantly higher values than those of the rest for the same traffic volume.

After identifying all points that had been rehabilitated, the SC related to them was excluded from the analysis. With the remaining data, a new mean SC was recalculated, obtaining a corrected SC ($SC_{corrected}$, Figure 3c). Now, we can assume that the corrected mean SC value is related to pavements in the equilibrium phase. Values before and after applying this methodology are presented in the Appendix A (Table A1).

Regarding the independent variables, AADT and AADT.HV were considered. In addition, in order to explore different possibilities that could better reproduce the data, we defined new coefficients that depend on AADT and AADT.HV. As AADT accounts for all heavy and light vehicles, we defined a new variable, AADT.LV, which only takes into account light vehicles. Even if it is well reported in the literature that heavy traffic affects pavement deterioration the most, we defined this parameter in order to see the possible effect of constant light traffic, as it could damage the pavement due to fatigue. AADT.LV was defined as shown in Equation (9):

$$\text{AADT.LV} = \text{AADT} - \text{AATD.HV} \quad (9)$$

The impact of each independent variable was evaluated using a forward-stepwise regression approach, implemented with SPSS software, Version 28.

5. Results and Discussions

To predict the MSSC, 66 segments with different traffic volumes were analyzed (Table 4), accounting for 366.560 m (32.3% of the single-carriageway road network). A multivariable regression analysis was conducted to derive an empirical equation linking the average MSSC on the roads of Gipuzkoa to various known influencing factors.

Firstly, an explanatory statistical analysis of the variables was performed (Table 5), which included the minimum, maximum, mean, and standard deviation of each variable considered.

Table 5. Explanatory statistical analysis of the variables.

Variable	Minimum	Maximum	Mean	Standard Deviation
MSSC	33.31	76.28	53.07	9.53
AADT	139	24,506	5499.73	5179.80
AADT.HV	7	3371.2	452.40	653.14
AADT.LV	130	23,771	5047.32	4769.05

Table 6 shows the correlations of the MSSC with the independent variables using Pearson's coefficient, R, as well as the *p*-values, of the correlations. The negative values of R show how increases in the AADT, AADT.HV, and AADT.LV lead to decreases in the value of the MSSC. All variables have a good correlation—over 0.50 in absolute values—and are significant (p-value < 0.05).

Table 6. Correlations of the dependent variable, MSSC, with the independent variables (Pearson coefficient, R).

Variables	R	*p*-Value
AADT	−0.554	<0.001
AADT.HV	−0.560	<0.001
AADT.LV	−0.525	<0.001

Transformations were applied to achieve a normal distribution of the independent variables. Table 7 shows the correlations of the MSSC with the different transformations proposed for the independent variables.

Table 7. Correlations of various transformations of AADT and AADT.HV with MSSC (R^2).

Type of Transformation	AADT (R^2)	AADT.HV (R^2)	AADT.LV (R^2)
Linear	0.306	0.314	0.275
Logarithm	0.378	0.382	0.364
Inverse	0.141	0.117	0.141
Quadratic	0.392	0.363	0.369
Cubic	0.423	0.417	0.413
Potential	0.369	0.390	0.352
Exponential	0.309	0.367	0.271

As shown in Table 6, AADT.HV achieved the highest correlation, followed by AADT, and, in last position, AADT.LV. Similarly, transformations were applied to all of the variables (Table 7) and only the inverse did not improve the linear correlation. Once again, considering the transformed variables, AADT.HV achieved the highest determination coefficients, followed by the other two variables, in the same order, for the Pearson's coefficient.

Among the different transformations proposed, the cubic transformation was not selected, despite exhibiting the best correlation with the MSSC. Typically, quadratic and cubic curves fit better but do not reproduce the pattern described in the literature. Usual trends relating skid resistance and traffic volumes show a negative pattern. An increase in the number of vehicles is reflected in a decrease in the available friction, as shown in Figure 2. Quadratic and cubic transformations could also produce this trend. However, when representing the solutions in a plot of the skid resistance vs. traffic volumes, some local maxima and minima can be observed, indicating that, for example, with a specific value of traffic volume lower friction is achieved than with higher volumes, implying an

inconsistency in the data. In fact, if we increase the degree of the proposed polynomial expression to a value of $n - 1$ (being n, the number of available data), a curve fitting of all of the points will be achieved but, logically, without a correct interpretation of the trend.

Next, using the independent variables and their corresponding transformations, various models were analyzed to predict summer friction (Table 8).

Table 8. Proposed MLR models.

Model	R^2	Notes
MSSC = Int + *AADT* + *AADT.HV*	0.372	All variables are significant.
MSSC = Int + *AADT* + Log*AADT.HV*	0.382	*AADT* is not significant.
MSSC = Int + Log*AADT* + *AADT.HV*	0.439	All variables are significant.
MSSC = Int + Log*AADT* + Log*AADT.HV*	0.382	Log*AADT.HV* is not significant.
MSSC = Int + Log*AADT* + $AADT.HV^2$	0.445	$AADT.HV^2$ is not significant.
MSSC = Int + $AADT^2$ + Log*AADT.HV*	0.386	$AADT^2$ is not significant.
MSSC = Int + Log*AADT* + Exp*AADT.HV*	0.436	Variables are not significant.
MSSC = Int + Log*AADT* + *AADT.HV* + Log*AADT.LV*	0.439	Log*AADT* is not significant

As can be seen in Table 8, the best model employs *AADT* and the logarithmic transformation of *AADT.HV*. As a result, Equation (10) is suggested for predicting skid resistance, with a 95% confidence interval.

$$\text{MSSC} = 83.661 - 8.138 \cdot \text{LogAADT} - 0.004 \cdot \text{AADT.HV} \quad (10)$$

where *AADT* and *AADT.HV* are expressed as vehicles/day and heavy vehicles/day, respectively. *MSSC* is the SC directly measured in the summer season, and it is expressed on a scale from 0 to 100. As can be seen in Equation (10), the logarithmic transformation of *AADT* appears to be particularly important for improving the model fit. The same does not hold true for the *AADT.HV* term, for which the linear component appears to provide the best fit for the model. Although the first skid-resistance-prediction model directly used traffic variables [43], other authors suggested the transformation of the traffic variables, such as exponential [59] or natural logarithms [55,56]. It seems that the daily traffic volumes do not proportionally polish the aggregates but tend toward an asymptotical value [51]. Moreover, it seems that those transformations allow for a normal distribution of the data, which are, generally, non-normally distributed, improving the correlation with the dependent variable.

The model's regression coefficient (R^2) is 0.439, suggesting that the equation accounts for almost 44% of the total variance across the 66 segments. The Durbin–Watson statistic of 1.845, between 1.5 and 2.5, confirms the independence of the residuals (Table 9). The variance influence factor (VIF) value of 1.522 indicates no collinearity issues.

Table 9. Analysis of variance (ANOVA) of Equation (10).

	Degrees of Freedom	Sum of Squares	Mean Squares	F	*p*-Value	Durbin–Watson
Model	2	2627.767	1313.884	24.631	<0.001	1.845
Residuals	63	3360.645	53.344			
Total	65	5988.412				

An F-test confirms the validity of the correlation ($p < 0.01$), while a Student's t-test analysis of the coefficients verifies that they are significant and distinct from zero (Table 10).

Table 10. Parameter estimates of Equation (10).

Variable	Parameter Estimates	Std. Error	t-Value	*p*-Value	Standardized Coefficient	95% Confidence Interval	
Intercept	83.661	7.268	11.511	<0.001		69.137	98.185
Log*AADT*	−8.138	2.174	−3.743	<0.001	−0.436	−12.483	−3.793
AADT.HV	−0.004	0.002	−2.619	0.011	−0.305	−0.008	−0.001

The dataset provides a reliable prediction model, yielding an R^2 value of 0.439. This value is near other determination coefficients presented in the literature [56,59,60]. The fact that this R^2 value is below values reported in other studies may be attributed to the fact that the influence of other factors affecting MSSC, such as PSV or surface material, has not been taken into account, as suggested in previous studies [28,40,43,55,59,60].

Figure 4 shows the predicted vs. observed values for Equation (10).

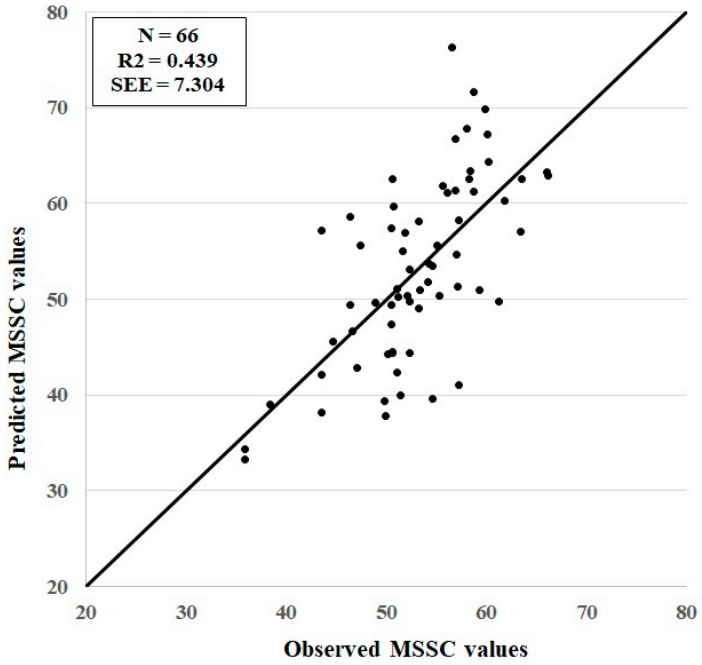

Figure 4. Predicted values vs. observed values for Equation (10).

Finally, Figure 5 provides a graphical representation of the expected MSSC values as a function of *AADT* and *AADT.HV* according to Equation (10). Different colors can be seen depending on the MSSC value. For low *AADT* and *AADT.HV* values, high MSSC values are expected, as low traffic volumes do not deteriorate the pavement as much, so friction values are high. On the other hand, when traffic volume increases, *MSSC* decreases. By fixing the number of light vehicles but increasing the number of heavy vehicles, we also see a considerable decrease in the *MSSC*. This clearly reflects the influence of heavy-vehicle traffic on SC, aligning well with the findings in previous research.

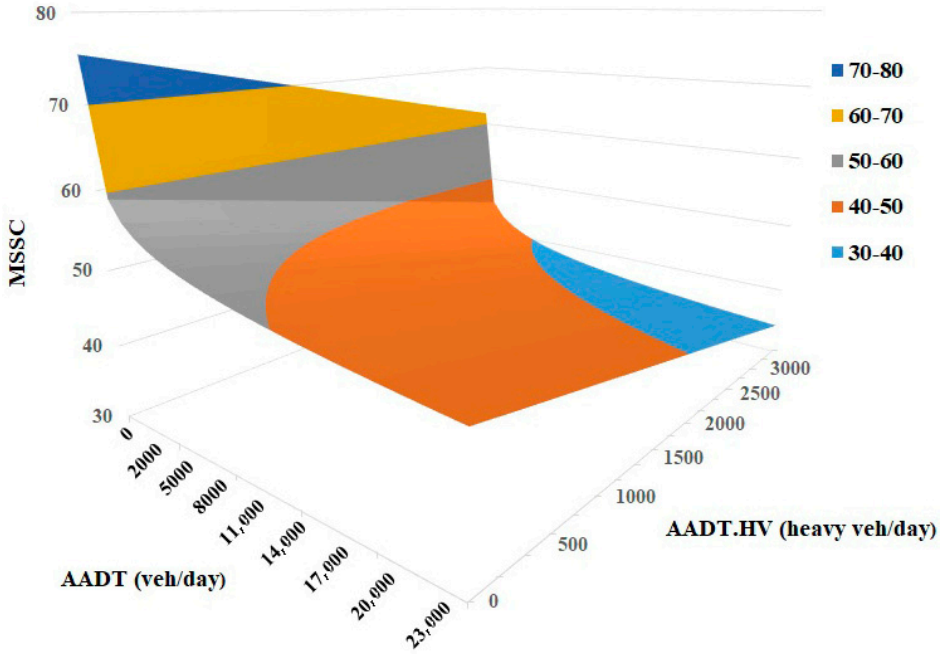

Figure 5. Expected SC values for various AADT and AADT.HV values according to Equation (10).

6. Conclusions

Due to the necessity of developing a model for predicting the available skid resistance on rural single-carriageway roads, for which there is, generally, a lack of detailed information about rehabilitation times and surface layer materials, this study analyzed SCRIM coefficient data collected in summer, when the coefficient is at its lowest value and, thus, road safety is more compromised. Including information about traffic volumes in a segment and adopting a new methodology to eliminate friction values for recently rehabilitated sub-segments, a skid-resistance-predicting model was developed with an R^2 of 0.439. Despite including only two variables as predictors, the annual average daily traffic (*AADT*) and the *AADT* of heavy vehicles (*AADT.HV*), an acceptable result was obtained. The model could benefit from additional variables, such as surface material or pavement-specific factors, whose absence limit the prediction accuracy. However, this simple but effective model provides a good approximation of the available friction in a specific segment in summer. This finding highlights the importance of including comprehensive information in pavement management systems to ensure that predictive models capture all relevant variables.

In summary, this work demonstrates that integrating additional information into pavement management systems is a crucial step toward developing robust and accurate predictive models that can support informed decision making in infrastructure management. More specifically, the inclusion of this model in the PMS workflows of the road authorities will enhance prediction capabilities for secondary roads, traditionally disregarded due to the variability in M&R treatments and the lack of detailed information in the database. Thus, this simplified but effective model makes it possible to identify segments of rural roads with low friction, indicating the areas that should be prioritized and monitored more closely.

Author Contributions: Conceptualization, H.P.-A., M.I., and I.G.; methodology, H.P.-A. and I.G.; software, H.P.-A., M.I., and Á.A.-S.; validation, H.P.-A., M.I., and Á.A.-S.; formal analysis, H.P.-A. and Á.A.-S.; investigation, H.P.-A. and I.G.; resources, M.I. and Á.A.-S.; data curation, H.P.-A., M.I., I.G., and Á.A.-S.; writing—original draft preparation, H.P.-A., M.I., and I.G.; writing—review and editing, H.P.-A., I.G., and Á.A.-S.; visualization, M.I. and Á.A.-S.; supervision, H.P.-A. and I.G.; project

administration, M.I. and I.G.; funding acquisition, H.P.-A., M.I., and I.G. All authors have read and agreed to the published version of the manuscript.

Funding: This research was funded by Gipuzkoako Foru Aldundia/Diputación Foral de Gipuzkoa, under grant number: P9, Project 'Gipuzkoan eraikuntza eta mugikortasun adimentsu eta jasangarria/Construcción y movilidad inteligentes y sostenibles en Gipuzkoa' of the Etorkizuna Eraikiz program 2022, and grant number: P10, Project 'MUGI JASS (MUgikortasuna Gipuzkoan: Interkonektatua, JASangarria eta Segurua/Movilidad en Gipuzkoa: interconectada, sostenible y segura)' of the Etorkizuna Eraikiz program 2024, as well as by the University of the Basque Country (UPV/EHU), under grant number: GIU21/046.

Data Availability Statement: The dataset is available at https://doi.org/10.5281/zenodo.15658703, accessed on 11 August 2025.

Conflicts of Interest: The authors declare no conflicts of interest.

Appendix A

Table A1. Data about the analyzed segments before and after filtering.

Seg.	Year	Length (km)	Before Filtering				After Filtering				Difference of Mean After Filtering
			Number of Data	Mean	Min.	Max.	Number of Data	Mean	Min.	Max.	
1	2021	6.100	590	38.86	20.69	67.47	468	34.37	20.69	49.22	4.49
2	2021	0.500	51	40.81	25.26	86.87	47	38.12	25.26	52.64	2.68
3	2021	1.020	102	4425	21.83	77.74	91	42.13	21.83	54.92	2.12
4	2021	5.540	573	38.27	22.97	68.62	455	33.31	22.97	48.08	4.96
5	2021	3.900	396	59.95	36.67	82.31	318	57.17	36.67	67.47	2.78
6	2021	15.100	1536	60.42	32.10	107.41	1303	58.12	33.24	68.62	2.30
7	2021	3.700	371	60.34	41.23	98.28	309	57.48	41.23	68.62	2.86
8	2021	4.900	494	58.84	34.38	94.86	425	56.90	35.53	66.33	1.94
9	2021	1.600	162	53.39	43.51	74.32	135	50.36	43.51	60.63	3.03
10	2021	0.500	50	53.76	37.81	70.90	41	51.08	37.81	61.77	2.68
11	2021	1.200	112	51.99	33.24	70.90	93	49.41	33.24	60.63	2.57
12	2021	3.100	315	52.77	28.68	83.45	278	50.97	28.68	61.77	1.80
13	2021	11.200	1132	56.40	32.10	93.72	950	53.53	32.10	65.19	2.87
14	2021	8.700	885	52.52	24.12	77.74	755	50.27	27.54	60.63	2.25
15	2021	3.600	370	52.58	30.96	103.99	309	49.64	30.96	61.77	2.94
16	2021	0.600	56	48.59	37.81	58.35	43	46.72	37.81	52.64	1.86
17	2021	2.500	253	57.94	35.53	82.31	215	55.65	35.53	66.33	2.29
18	2021	1.300	121	59.17	30.96	89.15	109	58.66	36.67	66.33	0.51
19	2021	3.900	453	51.92	28.68	75.46	388	49.37	28.68	62.91	2.56
20	2021	3.900	485	50.25	32.10	78.88	407	47.33	32.10	59.49	2.92
21	2021	11.200	284	44.24	25.26	90.29	258	42.36	25.26	52.64	1.87
22	2021	15.100	301	53.77	28.68	108.55	260	49.04	28.68	67.47	4.72
23	2021	1.000	110	44.49	34.38	92.58	208	42.80	34.38	53.78	1.69
24	2021	1.400	131	47.12	35.53	92.58	119	45.53	35.53	53.78	1.59
25	2019	2.500	246	42.37	27.38	76.45	203	39.60	27.38	49.06	2.76
26	2019	2.200	227	55.13	31.95	70.74	192	53.08	31.95	63.90	2.05
27	2020	13.200	706	66.91	30.81	135.78	596	63.33	30.81	78.73	3.59
28	2020	2.500	15	50.81	47.92	57.05	14	50.37	47.92	52.49	0.45
29	2019	7.900	805	65.86	33.09	100.41	681	62.56	33.09	77.59	3.30
30	2019	3.700	376	60.40	3423	83.29	321	58.27	37.65	68.46	2.13
31	2019	4.400	443	78.06	35.37	106.12	386	76.28	42.22	90.14	1.78
32	2019	4.000	407	57.94	34.23	92.42	339	54.65	34.23	67.32	3.29
33	2019	7.000	721	54.92	29.67	100.41	600	51.28	29.67	65.04	3.64
34	2019	3.400	415	41.52	19.40	63.90	351	39.34	19.40	49.06	2.18
35	2019	5.100	538	41.27	11.41	57.05	475	39.92	17.12	49.06	1.35
36	2019	0.300	30	42.22	28.53	54.77	23	39.04	28.53	46.78	3.17
37	2019	9.400	955	57.68	33.09	95.85	839	55.65	33.09	67.32	2.03
38	2019	8.100	823	64.05	29.67	99.27	711	61.79	34.23	74.17	2.26
39	2019	8.500	861	71.01	33.09	112.96	726	66.76	33.09	84.44	4.25
40	2019	0.700	70	45.85	34.23	57.05	59	44.40	34.23	50.21	1.45
41	2019	10.000	1601	48.66	19.40	93.56	1315	44.26	19.40	60.47	4.40

Table A1. *Cont.*

Seg.	Year	Length (km)	Before Filtering				After Filtering				Difference of Mean After Filtering
			Number of Data	Mean	Min.	Max.	Number of Data	Mean	Min.	Max.	
42	2019	2.600	264	54.83	34.23	93.56	210	49.75	34.23	66.18	5.09
43	2019	6.100	618	66.96	37.65	104.97	510	63.41	37.65	77.59	3.55
44	2019	3.800	386	50.13	28.53	77.59	297	44.47	28.53	61.62	5.66
45	2019	5.000	515	63.83	36.51	103.83	453	61.16	36.51	74.17	2.67
46	2019	4.300	443	39.92	23.96	68.46	380	37.78	23.96	46.78	2.14
47	2019	6.400	653	72.78	33.09	104.97	562	69.84	33.09	84.44	2.94
48	2019	7.100	729	71.64	44.50	103.83	589	67.78	44.50	82.15	3.86
49	2020	5.400	551	57.96	18.26	81.01	469	57.03	28.53	68.46	0.93
50	2020	10.100	16	64.33	55.91	73.03	13	62.58	55.91	68.46	1.74
51	2020	6.700	686	64.51	37.65	95.85	578	61.35	37.65	75.31	3.16
52	2020	5.300	540	48.83	22.82	81.01	432	44.41	22.82	59.33	4.42
53	2020	4.500	264	63.40	29.67	77.59	404	62.55	29.67	69.60	5.09
54	2020	8.700	306	52.98	21.68	90.14	264	49.80	21.68	63.90	3.18
55	2020	19.100	332	46.07	19.40	90.14	275	41.06	19.40	60.47	5.01
56	2020	10.800	177	65.31	44.50	84.44	151	62.98	44.50	74.17	2.33
57	2020	4.500	458	62.71	28.53	119.81	419	61.26	28.53	74.17	1.45
58	2020	0.700	75	62.00	52.49	75.31	60	59.64	52.49	67.32	2.36
59	2020	0.500	52	56.48	43.36	70.74	44	55.00	43.36	60.47	1.48
60	2020	4.300	439	69.25	35.37	101.55	377	67.25	43.36	77.59	2.00
61	2020	9.000	914	63.03	29.67	91.28	778	60.28	33.09	73.03	2.75
62	2020	3.000	298	57.17	34.23	79.87	241	53.73	34.23	67.32	3.44
63	2020	9.300	949	55.23	29.67	93.56	790	50.96	29.67	67.32	4.27
64	2020	11.700	1189	72.87	34.23	99.27	1017	71.59	50.21	79.87	1.28
65	2020	4.000	410	55.75	35.37	86.72	337	51.76	35.37	66.18	3.99
66	2020	9.200	403	67.62	45.64	95.85	329	64.33	45.64	76.45	3.29
	TOTAL	366.500	MEAN	55.67			MEAN	53.07		MEAN	2.79

References

1. Fernandes, A.; Neves, J. Threshold Values of Pavement Surface Properties for Maintenance Purposes Based on Accidents Modelling. *Int. J. Pavement Eng.* **2014**, *15*, 917–924. [CrossRef]
2. Wang, D.; Chen, X.; Yin, C.; Oeser, M.; Steinauer, B. Influence of Different Polishing Conditions on the Skid Resistance Development of Asphalt Surface. *Wear* **2013**, *308*, 71–78. [CrossRef]
3. Tamagusko, T.; Gomes Correia, M.; Ferreira, A. Machine Learning Applications in Road Pavement Management: A Review, Challenges and Future Directions. *Infrastructures* **2024**, *9*, 213. [CrossRef]
4. Ban, I.; Deluka-Tibljaš, A.; Ruži'c, I.R. Skid Resistance Performance Assessment by a PLS Regression-Based Predictive Model with Non-Standard Texture Parameters. *Lubricants* **2024**, *12*, 23. [CrossRef]
5. Pérez-Acebo, H.; Ziolkowski, R.; Gonzalo-Orden, H. Evaluation of the Radar Speed Cameras and Panels Indicating the Vehicles' Speed as Traffic Calming Measures (TCM) in Short Length Urban Areas Located Along Rural Roads. *Energies* **2021**, *14*, 8146. [CrossRef]
6. Llopis-Castelló, D.; Findley, D.J. Influence of Calibration Factors on Crash Prediction on Rural Two-Lane Two-Way Roadway Segments. *J. Transp. Eng. A Syst.* **2019**, *145*, 04019024. [CrossRef]
7. Chen, Y.; Li, Y.; King, M.; Shi, Q.; Wang, C.; Li, P. Identification Methods of Key Contributing Factors in Crashes with High Numbers of Fatalities and Injuries in China. *Traffic Inj. Prev.* **2016**, *17*, 878–883. [CrossRef] [PubMed]
8. Hall, J.W.; Smith, K.L.; Titus-Glover, L.; Wambold, J.C.; Yager, T.J.; Rado, Z. *Guide for Pavement Friction National Cooperative Highway Research Program NCHRP Project 01-43*; Transportation Research Board: Washington, DC, USA, 2009.
9. Lyon, C.; Persaud, B. Safety Effects of Targeted Program to Improve Skid Resistance. *Transp. Res. Rec.* **2008**, *2068*, 135–140. [CrossRef]
10. AASHTO. *Pavement Management Guide*, 2nd ed.; AASHTO: Washington, DC, USA, 2012.
11. Buddhavarapu, P.; Banerjee, A.; Prozzi, J.A. Influence of Pavement Condition on Horizontal Curve Safety. *Accid. Anal. Prev.* **2013**, *52*, 9–18. [CrossRef]
12. Ongel, A.; Lu, Q.; Harvey, J. Frictional Properties of Asphalt Concrete Mixes. *Proc. Inst. Civ. Eng. Transp.* **2009**, *162*, 19–26. [CrossRef]
13. Cafiso, S.; Montella, A.; D'Agostino, C.; Mauriello, F.; Galante, F. Crash Modification Functions for Pavement Surface Condition and Geometric Design Indicators. *Accid. Anal. Prev.* **2021**, *149*, 105887. [CrossRef]
14. Araujo, V.M.C.; Bessa, I.S.; Castelo Branco, V.T.F. Measuring Skid Resistance of Hot Mix Asphalt Using the Aggregate Image Measurement System (AIMS). *Constr. Build. Mater.* **2015**, *98*, 476–481. [CrossRef]

15. Abaza, K.A.; Murad, M.M. Prediction of Pavement Friction Using Markov Chain at the Project and Network Levels. *Int. J. Pavement Eng.* **2024**, *25*, 2371449. [CrossRef]
16. Papageorgiou, G.; Mouratidis, A. Defining Threshold Values for Pavement Surface Characteristics. *Proc. Inst. Civ. Eng. Transp.* **2015**, *168*, 223–230. [CrossRef]
17. Liu, Y.; Cheng, X.; Yang, Z. Effect of Mixture Design Parameters of Stone Mastic Asphalt Pavement on Its Skid Resistance. *Appl. Sci.* **2019**, *9*, 5171. [CrossRef]
18. Moaveni, M.; Mahmoud, E.; Ortiz, E.M.; Tutumluer, E.; Beshears, S. Use of Advanced Aggregate Imaging Systems to Evaluate Aggregate Resistance to Breakage, Abrasion, and Polishing. *Transp. Res. Rec.* **2014**, *2401*, 1–10. [CrossRef]
19. Peng, Y.; Li, J.Q.; Zhan, Y.; Wang, K.C. Finite Element Method-Based Skid Resistance Simulation Using In-Situ 3D Pavement Surface Texture and Friction Data. *Materials* **2019**, *12*, 3821. [CrossRef]
20. Permanent International Association of Road Congress (PIARC). Report of the Committee on Surface Characteristics. In Proceedings of the XVIII World Road Association, Brussels, Belgium, 13–19 September 1987.
21. Pérez-Acebo, H.; Isasa, M.; Gurrutxaga, I.; Alonso-Solórzano, Á. Analysis of the Skid Resistance Decrease in Bituminous Pavements in Dual-Carriageway Tunnels. *Buildings* **2024**, *14*, 3963. [CrossRef]
22. Gao, J.; Fan, J.; Gao, C.; Song, L. Friction Prediction in Asphalt Pavements: The Role of Separated Macro-and Micro-Texture Parameters Under Dry and Wet Conditions. *Lubricants* **2025**, *13*, 138. [CrossRef]
23. Wallman, C.-G.; Åström, H. *Friction Measurement Methods and the Correlation Between Road Friction and Traffic Safety. A Literature Review*; Swedish National Road and Transport Research Institute (VTI): Linköping, Sweden, 2001.
24. Edmondson, V.; Woodward, J.; Lim, M.; Kane, M.; Martin, J.; Shyha, I. Improved Non-Contact 3D Field and Processing Techniques to Achieve Macrotexture Characterisation of Pavements. *Constr. Build. Mater.* **2019**, *227*, 116693. [CrossRef]
25. Koné, A.; Es-Sabar, A.; Do, M.-T. Application of Machine Learning Models to the Analysis of Skid Resistance Data. *Lubricants* **2023**, *11*, 328. [CrossRef]
26. Highways England. *Design Manual for Roads and Bridges Pavement Inspection & Assessment CS 228 Skidding Resistance*; Highways England: London, UK, 2021.
27. Ministerio de Fomento. *Orden FOM/2523/2014, de 12 de Diciembre, por la Que se Actualizan Determinados Artículos del Pliego de Prescripciones Técnicas Generas Para Obras de Carreteras y Puentes, Relativos a Materiales Básicos, a Firmes y Pavimentos, y a Senalización, Balizamiento y Sistemas de Contención de Vehículos*; Ministerio de Fomento: Madrid, Spain, 2014.
28. Pérez-Acebo, H.; Gonzalo-Orden, H.; Rojí, E. Skid Resistance Prediction for New Two-Lane Roads. *Proc. Inst. Civ. Eng. Transp.* **2019**, *172*, 264–273. [CrossRef]
29. Kokkalis, A.G. Prediction of Skid Resistance from Texture Measurements. *Proc. Inst. Civ. Eng. Transp.* **1998**, *129*, 85–93. [CrossRef]
30. Kandji, M.; Fournier, B.; Duchesne, J.; Doucet, F. Effect of Polishing Time, Mechanisms and Mineralogy on the Microtexture Evolution and Polishing Resistance of Pavement Surface Aggregates. *Constr. Build. Mater.* **2025**, *476*, 141105. [CrossRef]
31. Jellie, J.H. *A Study of Factors Affecting Skid Resistance Characteristics*; University of Ulster: Jordanstown, UK, 2003.
32. Achútegi Viada, F. *Características Superficiales de los Firmes de Carretera*; Centro de Estudios de Experimentación de Obras Publicas CEDEX, Ed.; Ministerio de Fomento: Madrid, Spain, 2005.
33. Navarro, J.A.; Luzuriaga, S.; Arnáiz, J.; Ruiz, A. Bitumen Wearing Course and Resistance to Sliding. *Carreteras* **2011**, *180*, 37–51.
34. Woodward, W.D.H.; Woodside, A.R.; Jellie, J.H. Early and Mid Life SMA Skid Resistance. In Proceedings of the International Conference on Surface Friction, Christchurch, New Zealand, 1–4 May 2005.
35. Wilson, D.J. *An Analysis of the Seasonal and Short-Term Variation of Road Pavement Skid Resistance*; University of Auckland: Auckland, New Zealand, 2006.
36. Burchett, J.L.; Rizenbergs, R.L. Seasonal variations in the skid resistance of pavement in Kentucky. *Transp. Res. Rec.* **1979**, *788*, 6–14.
37. Echaveguren, T.; de Solminihac, H. Seasonal Variability of Skid Resistance in Paved Roadways. *Proc. Inst. Civ. Eng. Transp.* **2011**, *164*, 23–32. [CrossRef]
38. Rogers, M.P.; Gargett, T. A Skidding Resistance Standard for the National Road Network. *Highways Transp.* **1991**, *38*, 10–13.
39. Hosking, J.; Woodford, G. *Measurement of Skid Resistance Part II. Factors Affecting the Slipperiness of a Road Surface TRRL Laboratory Report 738*; Transport and Road Research Laoratory: Crowthorne, UK, 1976.
40. Salt, G.F. Research on Skid-Resistance at the Transport and Road Research Laboratory (1927–1977). *Transp. Res. Rec.* **1977**, *622*, 26–38.
41. Li, J.; Yu, J.; Xie, J.; Ye, Q. Performance Degradation of Large-Sized Asphalt Mixture Specimen under Heavy Load and Its Affecting Factors Using Multifunctional Pavement Material Tester. *Materials* **2019**, *12*, 3814. [CrossRef] [PubMed]
42. Kennedy, C.K.; Young, A.E.; Butler, I.C. Measurement of Skidding Resistance and Surface Texture and the Use of Results in the United Kingdom. *ASTM Spec. Tech. Publ.* **1990**, *STP1031-EB*, 87–102. [CrossRef]
43. Szatkowski, W.S.; Hosking, J.R. *The Effect of Traffic and Aggregate on the Skidding Resistance of Bituminous Surfacing TRRL Report LR 504*; Transport and Road Research Laboratory: Crowthorne, UK, 1972.

44. Haas, R.; Hudson, W.R.; Falls, L.C. *Pavement Asset Management*; John Wiley & Sons: Hoboken, NJ, USA, 2015.
45. Kulkarni, R.B.; Miller, R.W. Pavement Management Systems: Past, Present, and Future. *Transp. Res. Rec.* **2003**, *1853*, 65–71. [CrossRef]
46. Wu, Y.; Pang, Y.; Zhu, X. Evolution of Prediction Models for Road Surface Irregularity: Trends, Methods and Future. *Constr. Build. Mater.* **2024**, *449*, 138316. [CrossRef]
47. Gurrutxaga, I.; Alonso-Solórzano, Á.; Isasa, M.; Pérez-Acebo, H. IRI Performance Models for Flexible, Semi-Rigid and Composite Pavements in Double-Carriageway Roads. *Civ. Eng. J.* **2025**, *11*, 1712–1738. [CrossRef]
48. Pérez-Acebo, H.; Linares-Unamunzaga, A.; Abejón, R.; Rojí, E. Research Trends in Pavement Management during the First Years of the 21st Century: A Bibliometric Analysis during the 2000-2013 Period. *Appl. Sci.* **2018**, *8*, 1041. [CrossRef]
49. Justo-Silva, R.; Ferreira, A.; Flintsch, G.; De Blasiis, M.R. Review on Machine Learning Techniques for Developing Pavement Performance Prediction Models. *Sustainability* **2021**, *13*, 5248. [CrossRef]
50. Echaveguren, T.; de Solminihac, H.; Chamorro, A. Long-Term Behaviour Model of Skid Resistance for Asphalt Roadway Surfaces. *Can. J. Civ. Eng.* **2010**, *37*, 719–727. [CrossRef]
51. Nicolosi, V.; D'Apuzzo, M.; Evangelisti, A.; Augeri, M. A New Methodological Approach for Road Friction Deterioration Models Development Based on Energetic Road Traffic Characterization. *Transp. Eng.* **2024**, *16*, 100251. [CrossRef]
52. Cenek, P.D.; Henderson, R.J.; Davies, R.B. *Selection of Aggregates for Skid Resistance*; NZ Transport Agency: Wellington, New Zealand, 2012.
53. Li, L.; Guler, S.I.; Donnell, E.T. Pavement Friction Degradation Based on Pennsylvania Field Test Data. *Transp. Res. Rec.* **2017**, *2639*, 11–19. [CrossRef]
54. Rith, M.; Kim, Y.K.; Lee, S.W. Characterization of Long-Term Skid Resistance in Exposed Aggregate Concrete Pavement. *Constr. Build. Mater.* **2020**, *256*, 119423. [CrossRef]
55. Pérez-Acebo, H.; Gonzalo-Orden, H.; Findley, D.J.; Rojí, E. A Skid Resistance Prediction Model for an Entire Road Network. *Constr. Build. Mater.* **2020**, *262*, 120041. [CrossRef]
56. Pérez-Acebo, H.; Montes-Redondo, M.; Appelt, A.; Findley, D.J. A Simplified Skid Resistance Predicting Model for a Freeway Network to Be Used in a Pavement Management System. *Int. J. Pavement Eng.* **2023**, *24*, 202066. [CrossRef]
57. Galvis Arce, O.D.; Zhang, Z. Skid Resistance Deterioration Model at the Network Level Using Markov Chains. *Int. J. Pavement Eng.* **2021**, *22*, 118–126. [CrossRef]
58. Fülöp, I.A.; Bogárdi, I.; Gulyás, A.; Csicsely-Tarpay, M. Use of Friction and Texture in Pavement Performance Modeling. *J. Transp. Eng.* **2000**, *126*, 243–248. [CrossRef]
59. Cenek, P.D.; Carpenter, P.; Jamieson, N.; Stewart, P. *Prediction of Skid Resistance Performance of Chip Seal Roads*; Research Report No. 256; Transfund New Zealand: Wellington, New Zealand, 2004.
60. WDM Ltd. *Investigation into the Relationship between Aggregate Polished Stone Value and Wet Skid Resistance*; Project PR3-0154; WDM Ltd.: Wellington, New Zealand, 1998.
61. Shamsaei, M.; Carter, A.; Vaillancourt, M. Using Construction and Demolition Waste Materials to Develop Chip Seals for Pavements. *Infrastructures* **2023**, *8*, 95. [CrossRef]
62. El-Ashwah, A.S.; Abdelrahman, M. Relating Aggregate Friction Properties to Asphalt Pavement Friction Loss through Laboratory Testing, Statistical Analysis, and Machine Learning Insights. *Int. J. Pavement Eng.* **2025**, *26*, 2456739. [CrossRef]
63. Meng, Y.; Chen, Z.; Wang, Z. Evaluating the Anti-Skid Performance of Asphalt Pavements with Basalt and Limestone Composite Aggregates: Testing and Prediction. *Buildings* **2024**, *14*, 2339. [CrossRef]
64. Chen, B.; Xiong, C.; Li, W.; He, J.; Zhang, X. Assessing Surface Texture Features of Asphalt Pavement Based on Three-Dimensional Laser Scanning Technology. *Buildings* **2021**, *11*, 623. [CrossRef]
65. Dai, G.; Luo, Z.; Chen, M.; Zhan, Y.; Ai, C. Reconstruction and Intelligent Evaluation of Three-Dimensional Texture of Stone Matrix Asphalt-13 Pavement for Skid Resistance. *Lubricants* **2023**, *11*, 535. [CrossRef]
66. Xu, G.; Lin, X.; Wang, S.; Zhan, Y.; Liu, J.; Huang, H. Incep-FrictionNet-Based Pavement Texture Friction Level Classification Prediction Method. *Lubricants* **2024**, *12*, 8. [CrossRef]
67. Yang, G.; Chen, K.-T.; Wang, K.; Li, J.; Zou, Y. Field Study of Asphalt Pavement Texture and Skid Resistance under Traffic Polishing Using 0.01 Mm 3D Images. *Lubricants* **2024**, *12*, 256. [CrossRef]
68. Zhan, Y.; Nie, Z.; Lin, X.; Zhang, A.A.; Ai, C. Hybrid Prediction Model for the Friction Performance of Asphalt Pavements by Combining Multi-Scale Decomposition and Transformer Network. *Eng. Appl. Artif. Intell.* **2025**, *155*, 110896. [CrossRef]
69. Aretoulis, N.; Liu, X.; Yin, C. 3D Reconstruction of Asphalt Pavement Macro-Texture Based on Convolutional Neural Network and Monocular Image Depth Estimation. *Appl. Sci.* **2025**, *15*, 4684. [CrossRef]
70. Wang, G.; Wang, K.C.P.; Yang, G. Intelligent Evaluation of Pavement Friction at High Speeds with Artificial Intelligence Powered Three-Dimensional Laser Imaging Technology. *Eng. Appl. Artif. Intell.* **2025**, *150*, 110580. [CrossRef]
71. Departamento de Infraestructuras Viarias y Estrategia Territorial. *Información de Aforos En Las Carreteras de Gipuzkoa Hasta 2023*; Diputación Foral de Gipuzkoa/Gipuzkoako Foru Aldundia: Donostia-San Sebastián, Spain, 2023.

72. Ministerio de Fomento. *FOM/3460/2003, de 28 de Noviembre, Por La Que Se Aprueba La Norma 6.1-IC "Secciones de Firme", de La Instrucción de Carreteras*; Ministerio de Fomento: Madrid, Spain, 2003.
73. Pérez-Acebo, H.; Gonzalo-Orden, H.; Findley, D.J.; Rojí, E. Modeling the International Roughness Index Performance on Semi-Rigid Pavements in Single Carriageway Roads. *Constr. Build. Mater.* **2021**, *272*, 121665. [CrossRef]
74. AENOR. *AENOR UNE-CEN/TS-15901-7:2010. Características Superficiales de Carreteras y Aeropuertos. Parte 7: Procedimiento Para 588 Determinar La Resistencia Al Desliza-Miento de La Superficie de Un Pavimento Utilizando Un Equipo Con El Ratio de De- 589 Slizamiento Longitudinal Fijo (CRLG): GripTester*; AENOR: Madrid, Spain, 2010.
75. Mohammadi, A.; Amador-Jimenez, L.; Elsaid, F. Simplified Pavement Performance Modeling with Only Two-Time Series Observations: A Case Study of Montreal Island. *J. Transp. Eng. Part B Pavements* **2019**, *145*, 05019004. [CrossRef]
76. Alonso-Solorzano, A.; Perez-Acebo, H.; Findley, D.J.; Gonzalo-Orden, H. Transition Probability Matrices for Pavement Deterioration Modelling with Variable Duty Cycle Times. *Int. J. Pavement Eng.* **2023**, *24*, 2278694. [CrossRef]
77. Abdelaziz, N.; Abd El-Hakim, R.T.; El-Badawy, S.M.; Afify, H.A. International Roughness Index Prediction Model for Flexible Pavements. *Int. J. Pavement Eng.* **2020**, *21*, 88–99. [CrossRef]
78. Osorio-Lird, A.; Chamorro, A.; Videla, C.; Tighe, S.; Torres-Machi, C. Application of Markov Chains and Monte Carlo Simulations for Developing Pavement Performance Models for Urban Network Management. *Struct. Infrastruct. Eng.* **2018**, *14*, 1169–1181. [CrossRef]
79. Deng, H. Traffic-Forecasting Model with Spatio-Temporal Kernel. *Electronics* **2025**, *14*, 1410. [CrossRef]
80. Pérez-López, C. *Técnicas Estadísticas Predictivas Con IBM SPSS*; Ibergaceta Publicaciones S.L.: Madrid, Spain, 2014.
81. Khasawneh, M.A. Laboratory Study on the Frictional Properties of HMA Specimens Using a Newly Developed Asphalt Polisher. *Int. J. Civ. Eng.* **2017**, *15*, 1007–1017. [CrossRef]
82. Rezaei, A.; Masad, E. Experimental-Based Model for Predicting the Skid Resistance of Asphalt Pavements. *Int. J. Pavement Eng.* **2013**, *14*, 24–35. [CrossRef]